Order online now!

www.rockland.com
tech@rockland.com
+1 484.791.3823

Datasheet for MB-070

Blocking Buffer for Fluorescent Western Blotting

Overview

Description:	Blocking Buffer for Fluorescent Western Blotting - MB-070
Item No.:	MB-070
Size:	500 mL
Applications:	WB, Cellular Assay, ELISA, IF, IHC, IP, Microarray, Other

Product Details

Background:	This blocking buffer is specifically designed for Western blotting using fluorochrome conjugated antibodies. Pure nitrocellulose membrane is recommended for maximum performance. Other membranes, such as PVDF or nitrocellulose embedded in a support can be used, but may generate elevated backgrounds. Protein should be transferred from gel to membrane using standard protocols. Blocking buffer can be used for membrane blocking and to dilute both primary and secondary antibodies. Blocking Buffer for Fluorescent Western Blotting is suitable for use with imaging systems produced by Bio-Rad Laboratories, GE Healthcare, Alpha Innotech, FujiFilm Life Science, Licor Biosciences, UVP and Syngene.
Synonyms:	Multiplex Blocking Buffer, Fluorescent Blocking Buffer, Blocking Solution, Blocking Buffer Western Blot, IRDye Western Blot Blocking Buffer, Alexa Dye Blocking Buffer, DyLight Blocking Buffer

Target Details

Purity/Specificity:	Blocking buffer was prepared using ultra pure reagents dissolved in pharmaceutical grade water (WFI) and consists of a proprietary protein formulation in TRIS buffered saline at pH 7.6 with thimerosal added as an antimicrobial agent.
Relevant Links:	• MB-070 SDS • PEPperCHIP Peptide Microarray Application Note

Application Details

Tested Applications:	WB
Suggested Applications:	Cellular Assay, ELISA, IF, IHC, IP, Microarray, Other (Based on references)

Application Note:	Fluorescence technology is widely used to detect proteins in both the visible and near-infrared ranges. This product allows for superior signal detection and lower background noise when fluorochrome conjugated antibodies are used to visualize proteins in Western blotting and other applications. Antibody conjugates prepared with IRDye® 800 and IRDye® 700DX, Cy2™, Cy3™, Cy3.5™, Cy5™ and Cy5.5™, DyLight™405, DyLight™ 549, DyLight™ 649, DyLight™ 680, and DyLight™ 800 and Alexa Fluor® 488, Alexa Fluor® 532, Alexa Fluor® 546, Alexa Fluor® 647 and Alexa Fluor® 680 have been validated on various platforms using this product with superior results compared to other commercially available products. In the infrared range, where little to no autofluorescence occurs, specific signal is sharply evident from any background giving the best possible signal-to-noise ratio. This allows for detection levels in the picogram range which rivals the sensitivity of chemiluminescence on film for Western blotting. Superior results are also seen when this product is used for simultaneous labeling (multiplex) in Western blots or microscopy using various fluorochrome combinations for multicolor imaging. Membranes blocked with this product can be dried and are very stable. Membranes that are stored protected from light can be re-washed and/or rescanned.
Assay Dilutions:	All assays should be optimized by the user. Recommended dilutions (if any) may be listed below.
WB:	User Defined

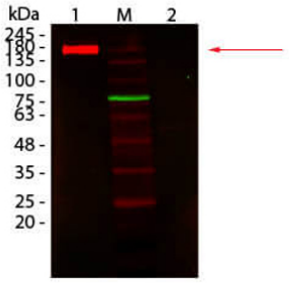
Formulation

Physical State:	Liquid (sterile filtered)
Concentration:	1 X
Buffer:	See application note.
Preservative:	Thimerosal is added as an antimicrobial agent.

Shipping & Handling

Shipping Condition:	Wet Ice
Storage Condition:	Store Blocking Buffer at 4° C prior to opening. DO NOT FREEZE.
Expiration:	Expiration date is six (6) months from date of receipt.

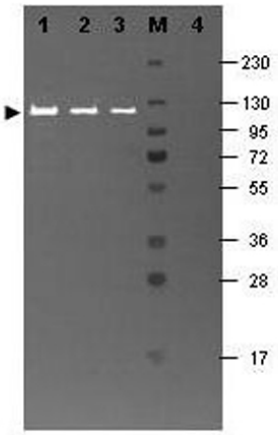
Images



Western Blot
Western Blot of Fluorescent TrueBlot®: Anti-Rabbit IgG DyLight 680 Conjugated using MB-070.
Lane 1: Rabbit IgG, Non-denatured.
Lane 2: Rabbit IgG, Denatured.
Load: 50 ng per lane.
Primary antibody: none.
Secondary antibody: Fluorescent TrueBlot®: Anti-Rabbit IgG DyLight 680 Conjugated antibody at 1:1,000 for 60 min at RT.
Block: MB-070 for 30 min at RT.
Predicted: 160 kDa for non-denatured; observed: 170-180 kDa for non-denatured. Band migrates at slightly higher molecular weight.



Western Blot
Multiplex western blot results using MB-070. Rockland Mouse-a-GST (200-301-200 lot 24882, blue), Rabbit anti-Transferrin (109-4134 lot 3033), and Goat-anti-Alpha-1-Anti-Trypsin (100-101-147 lot 5842) were used in a multiplex system to detect target proteins under reducing conditions in albumin depleted human serum with 320 ng of added GST. Sample was run by SDS-PAGE, transferred to 0.2 um PVDF using the BioRad Trans-Blot Turbo and blocked in 2.5% Blotto, 2.5% BSA, 0.02% Tween over night at 4°C. Membrane was probed with three primary antibodies at 1:1000 dilution (in MB-070 over night at 4°C). Detection shown was using DyLight™549 Donkey anti-Rabbit IgG (611-742-127 lot 21100, shown as green) DyLight™488 Donkey anti-Mouse IgG (610-741-124 lot 21095, shown as blue), and DyLight™649 Donkey anti-Goat IgG (605-743-125 lot 20834, shown as red) at 1:10,000 (in MB-070 at 30 min RT). Blots were washed, rinsed in methanol, dried and Images were collected using the BioRad VersaDoc System.



Western Blot
Western blot results using MB-070 and Fluorescein conjugated anti-b-Galactosidase antibody shows a band at ~117 kDa. Lanes 1 - 3 loaded with 60 ng, 30 ng and 15 ng, respectively of b-Gal present in partially purified preparations (arrowhead). Lane 4 shows no cross reactivity with proteins present in a non-specific control E.coli lysate. Proteins were resolved on a 4-20% Tris-Glycine gel by SDS-PAGE and transferred to nitrocellulose and blocking using Blocking Buffer for Fluorescent Western Blotting (p/n MB-070). The membrane was probed with fluorescein conjugated anti-b-Galactosidase (p/n 200-4236) diluted to 1:10,000. Reaction occurred for 2 hours at room temperature. Molecular weight estimation was made by comparison to a prestained MW marker in lane M. Fluorescence image was captured using the VersaDoc® Imaging System developed by BIO-RAD. Other detection systems will yield similar results.



Dot Blot
Dot Blot of Human IgA Fluorescein using MB-070.
Antigen: Human IgA Fluorescein.
Load: 3-fold serial dilution starting at 200 ng.
Block: MB-070 for 30 min at RT.

Example of stained microarray

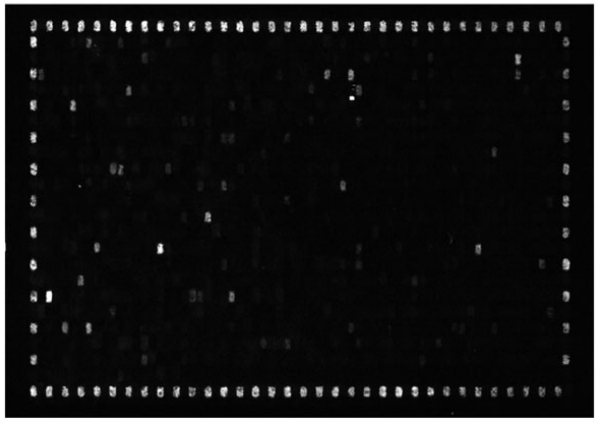
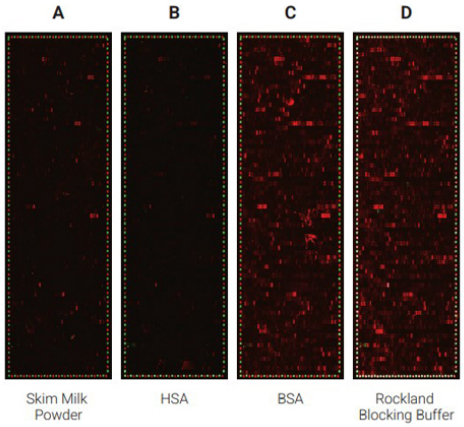
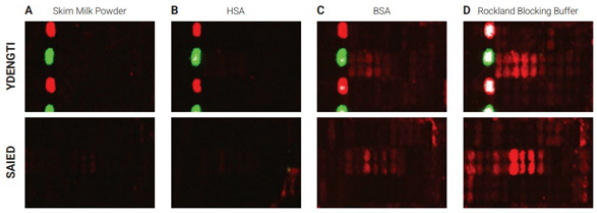


Figure
702 Peptides are printed in duplicates randomly distributed on the microarray. Control peptides (HA and FLAG controls) are located in a square surrounding the peptides of interest. As secondary antibody DyLight™ 549 conjugated goat anti-human IgG antibody and for the FLAG control peptide a mouse anti-FLAG-Cy3 antibody were used; microarrays were read using a Fujifilm Life Science FLA-5100 imaging system with a SHG 532nm (green) diode laser and an LPG filter. Fig e1. PMID: 26894206.



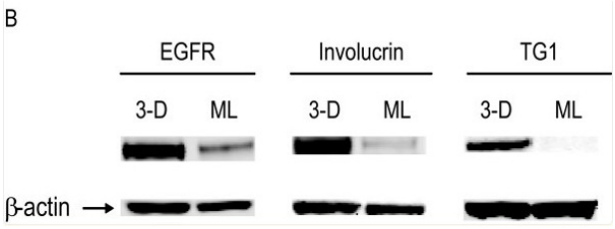
Comparison of the performance of different blocking reagents in epitope mappings with PEPperCHIP® Peptide Microarrays.
The PEPperCHIP® Peptide Microarrays were blocked for 30 minutes with either 2% skim milk powder (A), 1% HSA (B), 1% BSA (C) or 100% Rockland Blocking Buffer [p/n MB-070] (D). A human serum sample was assayed at dilution 1:200, followed by detection with secondary goat anti-Human IgG (H+L) DyLight™ 680 Antibody [p/n 609-144-123] and a control anti-HA (12CA5)-DyLight™ 800 Antibody. Red spots = sample IgG response and frame of polio control peptides, green spots = frame of HA control peptides.



Selected sections of the PEPperCHIP® Peptide Microarrays after assay with different blocking reagents. The microarrays were blocked for 30 minutes with either 2% skim milk powder (A), 1% HSA (B), 1% BSA (C) or 100% Rockland Blocking Buffer [p/n MB-070] (D), respectively. A human serum sample was assayed at dilution 1:200, followed by detection with secondary goat Anti-Human IgG (H+L) DyLight™ 680 Antibody [p/n 609-144-123]. Red spots = sample responses and polio control peptides, green spots = HA control peptides. The underlying binding motifs of the respective sections are indicated on the left.



Bottle
Blocking Buffer for Fluorescent Western Blotting



Western Blot
Expression of corneal epithelial gene markers. (B) The relative protein expression levels of EGFR (p/n 100-401-149), involucrin and TG1 as determined by Western blot assay; β-actin (p/n 600-401-886) was used as a loading control. Fig 3. PMID: 19638217

References

- Walaas GAE et al. Patient-matched transcriptomics of in vivo and in vitro colonic epithelium substantiate organoids as a translational model for ulcerative colitis. *Sci Rep.* (2026)
- Do HTT et al. HyperTRIBE identifies hepatic IGF2BP2/IMP2 targets in vivo and links IMP2 to autophagy. *NAR Mol Med.* (2026)
- Watanabe R et al. Repositioning of polyubiquitin alters the pathologic tau filament structure. *Nat Struct Mol Biol.* (2026)
- Schymik HS et al. IGF2BP2 Deficiency in Macrophages Impairs Migration, Reprograms Metabolism, and Limits Tumor Progression. *Int J Biol Sci.* (2026)
- Massey N et al. Kv1.3 as an upstream regulator of oxidative stress-mediated neuroinflammation following organic dust exposure in murine in vitro, ex vivo, and in vivo models. *Front Toxicol.* (2026)
- Vazaios K et al. Boosting CAR T cell functionality with oncolytic viruses for the treatment of pediatric diffuse midline gliomas. *Mol Ther Oncol.* (2026)
- da Silva Borges JV et al. System-wide immunoregulation by polyvalent IgG: integrating transcriptomic, miRNA, and proteomic landscapes. *J Transl Med.* (2026)
- Ramirez JJ et al. Astrocyte-microglia crosstalk through Hevin and Toll-like receptor signaling controls developmental thalamocortical synapse refinement. *Neuron.* (2026)
- Wan XF et al. Epitope-spanning antigenic variation reprograms immunodominance and broadens immunity in sequential influenza vaccination. *Nat Commun.* (2026)
- Moreira ALB et al. SARS-CoV-2-Induced IgG Repertoires Shape Gamma-Delta T Cell Responses: Evidence for Direct IgG-Membrane Interaction According to Disease Severity. *Cells.* (2026)
- Cell Rep Methods. Development of motif-specific monoclonal antibodies for global protein citrullination detection with minimal cross-reactivity to homocitrullination. *Laposchan S et al.* (2026)
- Morichon L et al. Human iPSC-derived airway models enable comparative analysis of SARS-CoV-2 infection in healthy and COPD bronchial epithelium. *iScience.* (2026)

- Jadiya P et al. Genetic ablation of neuronal mitochondrial calcium uptake impedes Alzheimer's disease progression. *EMBO J.* (2026)
- Chen G et al. Evaluating the efficacy of Bemcentinib (BGB) in modulating Axl activity in the brain of the rNLS8 inducible mouse model of ALS. *Nature [Preprint].* (2026)
- Barazas M et al. A mutational scar-based genome-wide map of DNA double-strand break repair. *Nat Commun.* (2026)
- Cohen HM et al. MICU proteins facilitate calcium-dependent mitochondrial metabolon formation to regulate cellular energetics independently of MCU. *Nat Metab.* (2026)
- Muller J et al. GLYATL1 is associated with metabolic and epigenetic changes and with endocrine resistance in luminal breast cancer. *Clin Epigenetics.* (2025)
- Samarakoon Y et al. UNC119 regulates T-cell receptor signalling in primary T cells and T acute lymphocytic leukaemia. *Life Sci Alliance.* (2025)
- Sridhar A et al. Tofacitinib and budesonide treatment affect stemness and chemokine release in IBD patient-derived colonoids. *Sci Rep.* (2025)
- van der Horst SC et al. Replication-IDentifier links epigenetic and metabolic pathways to the replication stress response. *Nat Commun.* (2025)
- Bunting EL et al. Antisense oligonucleotide-mediated MSH3 suppression reduces somatic CAG repeat expansion in Huntington's disease iPSC-derived striatal neurons. *Sci Transl Med.* (2025)
- Machado NR et al. Deciphering the IgG Idiotype Network Through Proteomic Analysis of Potential Targets in SARS-CoV-2 -Induced Immune Responses. *Immunology.* (2025)
- Mondal J et al. Selective targeting of oncogenic KRAS G12D using peptide nucleic acid oligomers attached to cell-penetrating peptides. *bioRxiv [Preprint].* (2025)
- Ledford BT et al. Apolipoprotein E Deficiency Produces an Inflammatory Abdominal Aortic Aneurysm in a Rat Calcium Chloride-Induced Model. *J Surg Res.* (2025)
- McNabb HJ et al. Systematic analysis of the RGS2 degron reveals characteristics of substrate recognition by the F-box protein FBXO44. *J Biol Chem.* (2025)
- van den Heuvel A et al. A Splicing Variant in XPA Results in Delayed Onset of Clinical Features of Xeroderma Pigmentosum. *J Invest Dermatol.* (2025)
- Brennan L et al. Hypoxia-Driven Histone Modifications Govern Gene Regulation for Mature Eye Lens Formation. *Invest Ophthalmol Vis Sci.* (2025)
- Achilles S et al. N-glycans on SLC26A3 do not significantly alter plasma membrane or lipid raft trafficking, but appear to stabilize interdomain contacts to stimulate transport. *Am J Physiol Gastrointest Liver Physiol.* (2025)
- Rivera Rodríguez R et al. The dietary phytochemicals carnosic acid and sulforaphane regulate inflammatory markers in ulcerative colitis patient-derived colonoids. *Front Pharmacol.* (2025)
- Kardani A et al. Laminar Flow Alters EV Composition in HUVECs: A Study of Culture Medium Optimization and Molecular Profiling of Vesicle Cargo. *Small Methods.* (2025)
- Machado NR et al. Proteomic Profiling of Human Peripheral Blood Cell Targets of IgG Induced by SARS-CoV-2: Insights into Vaccine Safety. *Vaccines (Basel).* (2025)

- Gibb AA et al. Integrated Systems Biology Identifies Disruptions in Mitochondrial Function and Metabolism as Key Contributors to HFpEF. *JACC Basic Transl Sci.* (2025)
- Rodemer W et al. Network Dysfunction Precedes Neurodegeneration in a dox-Regulatable TDP-43 Mouse Model of ALS-FTD. *J Neurosci.* (2025)
- Culviner PH et al. Evolution of Mycobacterium tuberculosis transcription regulation is associated with increased transmission and drug resistance. *Cell.* (2025)
- Shukla S et al. Cell-type-specific dysregulation of mitochondrial calcium signaling in Alzheimer's disease. *Cell Commun Signal.* (2025)
- Bergamasco IS et al. IgG Idiotype Diversity Shapes Cytokine Profiles and Autoantibody Targets in HTLV-1 Clinical Outcomes. *Int J Mol Sci.* (2025)
- Anderson AP et al. A distinct PP2A subunit regulates local protein phosphorylation at the axon initial segment. *Nat Commun.* (2025)
- Uchiumi T et al. Development of a novel histidine-rich glycoprotein measurement system as a biomarker for sepsis. *J Immunol Methods.* (2025)
- Maloney MT et al. LRRK2 kinase activity regulates Parkinson's disease-relevant lipids at the lysosome. *Mol Neurodegener.* (2025)
- Lytton SD et al. Peptide Epitopes of NC16A BP180 in the Diagnostics of Bullous Pemphigoid. *JID Innov.* (2025)
- Campa MJ et al. A tumor-binding antibody with cross-reactivity to viral antigens. *Cancer Immunol Immunother.* (2025)
- de Oliveira AA et al. Excessive Hypercholesterolemia in Pregnancy Impairs Later-Life Maternal Vascular Function in Rats. *J Am Heart Assoc.* (2025)
- Sharma S et al. Macrophage Proangiogenic VEGF-A Is Required for Inflammatory Arteriogenesis During Vascular Injury. *Biomedicines.* (2025)
- Charli A et al. Mitochondrial stress disassembles nuclear architecture through proteolytic activation of PKCδ and Lamin B1 phosphorylation in neuronal cells: implications for pathogenesis of age-related neurodegenerative diseases. *Front Cell Neurosci.* (2025)
- Gomes FP et al. Native top-down proteomics enables discovery in endocrine-resistant breast cancer. *Nat Chem Biol.* (2025)
- Bailey JK et al. Initial Characterization of WDR5B Reveals a Role in the Proliferation of Retinal Pigment Epithelial Cells. *Cells.* (2024)
- Huang M et al. Mitochondrial stress-induced H4K12 hyperacetylation dysregulates transcription in Parkinson's disease. *Front Cell Neurosci.* (2024)
- Putra M et al. Inhibiting Inducible Nitric Oxide Synthase with 1400W Reduces Soman (GD)-Induced Ferroptosis in Long-Term Epilepsy-Associated Neuropathology: Structural and Functional Magnetic Resonance Imaging Correlations with Neurobehavior and Brain Pathology. *J Pharmacol Exp Ther.* (2024)
- Schmidt D et al. Selective peptide binders to the perfluorinated sulfonic acid ionomer nafion. *Advanced Functional Materials.* (2024)
- View More ...

www.rockland.com
tech@rockland.com
+1 484.791.3823

Disclaimer

This product is for research use only and is not intended for therapeutic or diagnostic applications. Please contact a technical service representative for more information. All products of animal origin manufactured by Rockland Immunochemicals are derived from starting materials of North American origin. Collection was performed in United States Department of Agriculture (USDA) inspected facilities and all materials have been inspected and certified to be free of disease and suitable for exportation. All properties listed are typical characteristics and are not specifications. All suggestions and data are offered in good faith but without guarantee as conditions and methods of use of our products are beyond our control. All claims must be made within 30 days following the date of delivery. The prospective user must determine the suitability of our materials before adopting them on a commercial scale. Suggested uses of our products are not recommendations to use our products in violation of any patent or as a license under any patent of Rockland Immunochemicals, Inc. If you require a commercial license to use this material and do not have one, then return this material, unopened to: Rockland Inc., P.O. BOX 5199, Limerick, Pennsylvania, USA.